PRE-PRINT
Emanuela Muscolino, Maria Assunta Costa, Maria Antonietta Sabatino, Sabina Alessi, Donatella Bulone, Pier Luigi San Biagio, Rosa Passantino, Daniela Giacomazza, Clelia Dispenza, Recombinant mussel protein Pvfp5β enhances cell adhesion of poly(vinyl alcohol)/k-carrageenan hydrogel scaffolds, International Journal of Biological Macromolecules, Volume 211, 2022, Pages 639-652, ISSN 0141-8130,
https://doi.org/10.1016/j.ijbiomac.2022.05.068.

Recombinant mussel protein Pvfp5β enhances cell adhesion of poly(vinyl alcohol)/k-carrageenan hydrogel scaffolds

Emanuela Muscolino[a,1], Maria Assunta Costa[b,1], Maria Antonietta Sabatino[a], Sabina Alessi[a], Donatella Bulone[b], Pier Luigi San Biagio[b], Rosa Passantino[b*], Daniela Giacomazza[b], Clelia Dispenza[ab]

[a]*Dipartimento di Ingegneria, Università degli Studi di Palermo, Viale delle Scienze, Edificio 6, 90128 Palermo, Italy*
[b]*Istituto di Biofisica, Consiglio Nazionale delle Ricerche, Via U. La Malfa, 153, 90146 Palermo, Italy*
[1]Both authors have contributed equally to this work and share first authorship.
*Corresponding author.
Postal address: Istituto di Biofisica, Consiglio Nazionale delle Ricerche, Via U. La Malfa, 153, 90146 Palermo, Italy
Telephone: +39 091 6809540
Fax: +39 091 6809349
E-mail address: rosa.passantino@cnr.it

Abstract

Polymeric hydrogels are increasingly considered as scaffolds for tissue engineering due to their extraordinary resemblance with the extracellular matrix (ECM) of many tissues. As cell adhesion is a key factor in regulating important cell functions, hydrogel scaffolds are often functionalized or loaded with a variety of bioactive molecules that can promote adhesion. Interesting biomimetic approaches exploit the properties of mussel-inspired recombinant adhesive proteins. In this work, we prepared hydrogel scaffolds with a 50 %w mixture of k-carrageenan (kC) and polyvinyl alcohol (PVA), by a two-step physical gelation process, and we coated them with *Perna viridis* foot protein-5β (Pvfp5β). The mechanical and morphological properties of hydrogels were investigated both after conditioning with typical cell culture media and also after coating with the Pvfp5β. The protein resulted strongly adsorbed onto the surface of the hydrogel and also able to penetrate in its interiors to a certain depth, mainly interacting with the kC component of the scaffold as resulted from confocal analysis. Mouse embryonic fibroblasts NIH-3T3 were seeded on top of the hydrogels and cultured up to two weeks. The role of Pvfp5β in promoting cell adhesion, spreading and colonization of the scaffold was demonstrated.

Keywords: Pvfp5β; Adhesive protein; EGF-like motifs; Poly(vinyl alcohol)/k-carrageenan; 3D scaffolds; Cell-laden.

1. Introduction

The reconstruction of damaged or missing human tissues requires proper scaffolds that can support cell growth. Polymeric hydrogels are increasingly considered as scaffolds for tissue engineering due to their fairly unique structure-derived properties. They are networks of hydrophilic polymer chains, where the crosslinking points can be either covalent bonds or physical interactions between functional groups or chain segments (hydrogen bonds, van der Waals interactions, crystalline domains, condensed hydrophobic domains). The polymeric network can incorporate and retain relatively large amounts of aqueous solutions and allow the exchange of oxygen, nutrients and catabolites with the external medium. Other distinctive features are the presence of a hierarchically structured porosity with dimensions spanning over different length scales, from nano to macro, large surface area, inherent flexibility, tunable mechanical strength and excellent biocompatibility. For these properties hydrogels can play the role of the ECM, promoting cell attachment, growth and differentiation, and gradually degrading or dissolving to allow their replacement with the engineered tissue. In order to control the various cellular processes, hydrogels are often functionalized or loaded with a spectrum of bioactive molecules, such as specific ligands for adhesion receptors on cells, growth factors, hormones, enzymes and other natural or synthetic regulators of cell behavior [1]. Cell adhesion is essential in cell communication and cell cycle regulation, hence of paramount importance in tissue engineering. To facilitate the adhesion of cells to the scaffold, biomimetic approaches have been explored. In particular, mussel adhesive proteins (MAPs) have attracted great attention as bio-adhesives in the medical field for their remarkable adhesion ability to both cells and various surfaces [2,3]. Mussels attach themselves to wet surfaces through the secretion of a protein-based water-resistant glue, composed of a mixture of MAPs or mussel foot proteins (mfps) [4,5]. The proteins confined to mussel adhesive plaques are mfp-2, -3, -4, -5, and -6. All these proteins contain an atypically high concentration of the catecholic amino acid, 3,4-dihydroxy-l-phenylalanine (DOPA), which is obtained by the post-translational enzymatic hydroxylation of tyrosine (Tyr) [6]. Indeed, DOPA is a key molecular moiety underlying

underwater mussel adhesion. DOPA-containing peptides are capable of versatile chemistries enabling them to stick to many different surfaces, either organic or inorganic, by establishing reversible, multiple noncovalent bonds, like hydrogen bonding, metal chelation, cation–π and π–π interactions [7,8]. Poly-ethylene glycol (PEG), hyaluronic acid (HA), alginate, poly-vinyl alcohol, etc., have been functionalized with catechols to provide adhesive, sealant, coating, and anchoring properties, particularly for biomedical applications [9,10,11]. However, growing evidence shows that the presence of DOPA alone is not a sufficient condition to generate strong underwater adhesion and the synergistic effect of catechol from DOPA and the adjacent lysine seems to be a determinant requirement. In salty water, lysine residues displace the hydrated cations from the mineral surface, leaving the underlying oxides free to bind DOPA [12].

Recently, the expression of the recombinant protein Pvfp5β containing unmodified Tyr was fine-tuned in *Escherichia coli*. It was demonstrated that this protein can also adsorb to both hydrophilic and hydrophobic surfaces [13]. The adhesion of Pvfp5β is comparable to the Pvfp5β with all Tyr modified in DOPA [14,15]. Surfaces coated with Pvfp5β are not toxic and improve cell adhesion and spreading of NIH-3T3 and HeLa cell lines [13].

Due to its half-ester sulphate moieties, kC is a strong anionic polymer and resembles the natural glycosaminoglycans (GAGs), which are an important component of the connective tissue. Blending kC with PVA allows obtaining composite scaffolds with higher, interconnected porosity, high swelling degree, improved toughness and degradability. PVA can be physically crosslinked by inducing the formation of crystalline domains via freeze-thawing.

In this study, hydrogel scaffolds were prepared by a two-step physical gelation process using a 50 %w mixture of kC and PVA. Both these polymers and their mixture dissolve in water at high temperature (ca. 80 °C). The gelation of kC is induced by cooling the mixture to room temperature and formation of crosslinks by chain association [16]. This first network entraps PVA-rich aqueous domains. In order to crosslink also PVA, a freeze-thawing treatment was then performed [17]. The swelling and erosion properties, mechanical properties and morphology of the hydrogel were preliminarily investigated. A functional coating with recombinant protein Pvfp5β was made by conditioning the hydrogel with a protein-containing water/acetic acid solution. The absorption and penetration of Pvfp5β onto

and into the hydrogel were assessed, as well as the impact of the coating on the viability, adhesion, proliferation of mouse embryonic fibroblasts (NIH-3T3).

2. Experimental

2.1 Materials

PVA powder, with a molecular weight of 146-186 kDa and a degree of hydrolysis greater than 99%, was supplied by Sigma-Aldrich; kC powder was provided by Gelcarin ME 8625 FCM BioPolymer; dibasic sodium phosphate (SFD), monobasic potassium phosphate (PFM) and NaCl were purchased from Sigma-Aldrich and used to prepare a buffered saline solution (PBS) with the following composition: SFD 0.111 %w, PFM 0.032 %w and NaCl 0, 85 %w; MilliQ® water was filtered with 0.22 micron membrane syringe filters before use; sodium azide (NaN_3) was purchased from Sigma-Aldrich and used as a preservative. DMEM (Dulbecco's Modified Eagle Medium) and DMEM supplemented with 10% bovine calf serum (BCS) (Sigma-Aldrich) were used as conditioning media.

2.2 Solution preparation

The solution containing PVA and kC were prepared at 6 %w total polymer concentration and 1:1 weight ratio of the two components. The mixture gently stirred at ca. 80 °C until complete homogenization (about 1 h). NaN_3 (0.02 %w) was added to the solutions used to prepare samples for the physicochemical and mechanical analyses, while for biological analyses the solutions were sterilized by autoclaving at 121°C for 20 min.

2.3 Hydrogel preparation

The solution was placed in 50 mm diameter glass petri dishes to obtain a liquid layer of about 2 mm thickness. Samples were then subjected to two freeze-thaw (FT) cycles, each consisting in 2 h dwell at -20 °C and 2 h dwell at room temperature. The systems

subjected to this thermal treatment are identified as “PVA3/kC3 FT1". From the 2 mm thick hydrogel films produced, 8 mm diameter disks were cut to perform swelling and erosion studies and 20 mm diameter disks for the rheological analysis.

2.4 Expression and purification of recombinant protein Pvfp5β

Recombinant protein Pvfp5β was expressed and purified as previously described [13] with some modifications. Briefly, the pht-Pvfp5β expression plasmid, encoding a hexa-histidine tag followed by a TEV cleavage site and Pvfp5β, was transformed into *E. coli* BL21-Gold(DE3) cells (Agilent Technologies). When A_{600} of the culture reached 0.6–0.8, expression was induced by 1 mM isopropyl-D-thiogalactopyranoside for 3 h at 37 °C and 250 rpm. The harvested cell pellet was washed twice with 100 mM Tris-HCl, 10 mM EDTA, 5 mM $CaCl_2$, pH 7.4 and then with 20 mM sodium phosphate buffer, pH 7.4. The cell pellet was resuspended in pre-chilled lysis buffer (20 mM sodium phosphate buffer, pH 7.4, 500 mM NaCl, 2 mM DTT) supplemented of 5 mM $MgCl_2$, complete, EDTA-free, protease inhibitor-Roche mixture, 10 µg/mL of DNase, and 0.5 mg/mL of lysozyme). The cells were disrupted on ice by ultrasonic homogenizer (Bandelin HD 2070) and incubated for 30 min at 4 °C. The inclusion bodies containing expressed recombinant Pvfp5β were washed twice in lysis buffer with 1% Triton X-100, followed by one wash in the same buffer. The washed inclusion bodies were solubilized for 2 h at room temperature then overnight at 4 °C in 8 M urea, 1 M NaCl, 2mM DTT, 20mM sodium phosphate buffer, pH 7.4). The supernatant was collected after centrifugation at 20,000 x g, 4 °C for 30 min, filtered using 0.45µm filter (Sartorius Stedim Biotech), and loaded onto a 5-mL HisTrap FF crude column prepacked with Ni-Sepharose (GE Healthcare Life Sciences) equilibrated in the same buffer of the protein sample. The His-tagged protein was eluted under denaturing and reducing conditions with a linear gradient from 0 to 500 mM of imidazole in 10 CV at room temperature. Refolding of the eluted protein was then performed by sequential extensive dialysis at 4 °C, first in 100 mM sodium acetate (pH 5.6), 2 mM reduced gluthatione (GSH), and 0.5 mM oxidized glutathione (GSSG), then in the same buffer with no GSH and GSSG. Last, refolded Pvfp5β was dialyzed in 5% acetic acid and lyophilized. Protein purity was assessed by

Sodium Dodecyl Sulphate - PolyAcrylamide Gel Electrophoresis (SDS-PAGE) and Coomassie Blue staining. Protein concentration was measured by spectrophotometric determination at 280 nm (extinction coefficient (ε) = 27570 M^{-1} cm^{-1}).

2.5 PVA3/kC3 FT1 hydrogel coating with Pvfp5β

Cylinder-shaped scaffolds (Ø 5 mm x 1 mm) were obtained from sterile 50 mm diameter hydrogel films by using aseptically a sharp punch. Hydrogel scaffolds were placed into a sterile 96-well tissue culture plate filled with 120 μL of 0.16 mg/mL Pvfp5β solution, which was prepared diluting the Pvfp5β dissolved in 5% acetic acid with Milli-Q water. After incubation at room temperature for 16–20 h, the solution was collected and the non-adsorbed Pvfp5β in the incubation medium was quantified by bicinchoninic acid (BCA) Protein Assay Kit (Pierce, Bonn, Germany), according to the manufacturer's instructions using the microplate procedure (10 μl sample/200 μl BCA working reagent; 37 °C/30 min; 560 nm). Its integrity was evaluated by SDS-PAGE and Coomassie Blue staining. Protein-coated hydrogel scaffolds, named after "PVA3/kC3 FT1-Pvfp5β" were thoroughly rinsed with sterile Milli-Q water to remove any unbound protein. The protein coating was visualized by Coomassie Blue staining. Hydrogel scaffolds treated with only solvent were used as negative control (uncoated).

2.6 Swelling and erosion experiments and medium uptake and retention analysis

Swelling and erosion measurements were performed using a large excess of PBS at 37 °C (V_{sample}/V_{PBS} =0.02). Conditioning medium uptake and retention measurements were carried out using DMEM (D) and DMEM supplemented with 10% BCS (D+S). The swelling tests in the media were carried out by immersing hydrogel discs cut from the films in ca. 1 mL of culture medium at 37 °C (V_{sample}/V_{medium}~0.16). All swelling/conditioning media contain also 0.02-0.05 %w NaN_3 as preservative. Samples were pre-weighed with a precision balance and immersed in the media, then taken from the solution after predetermined time intervals, carefully dried and weighed. The

solvent was not changed or replenished during the experiment. The percentage mass change (%MC) is defined as:

$$\%MC = \frac{W_s - W_i}{W_i} \times 100 \quad (1)$$

where, Wi is the initial weight of the hydrogel and Ws is the weight of the swollen hydrogel, at the time interval TX, where X indicates the number of days and X=0 refers to the "as prepared" system.

2.7 Rheological analysis in small-oscillatory conditions

The rheological characterization was performed using a stress-controlled rheometer, AR G2, TA Instruments. The geometry used was the acrylic plate-plate (20 mm diameter). The samples were placed directly on the fixed plate of the instrument, previously set at the temperature of 37 ± 1°C.

Strain sweep tests were performed at constant frequency of 1 Hz in the 0.0001-0.01 strain range. Frequency sweep tests were performed in the 0.01-50 Hz frequency range by selecting, for each material, a constant strain value within the linear viscoelastic region, as determined by preliminary strain sweep tests. Samples were previously immersed in DMEM and DMEM supplemented with 10% BCS for TX days.

2.8 Morphological Analysis

2.8.1 Scanning electron microscopy

The morphological analysis of the samples was performed using a desktop Phenom ProX Scanning Electron Microscope (SEM) at an acceleration voltage of 10 kV.

The samples subjected to morphological analysis via SEM were the as prepared hydrogels, hydrogels incubated for 24 h in 0.6 %v acetic acid solution and incubated in 0.6 %v acetic acid solution with 0.16 mg/mL Pvfp5β. Incubation was performed at room temperature. Samples were then frozen in liquid nitrogen and lyophilized, then cut transversely mounted on aluminum stubs by means of an adhesive layer of colloidal

silver to expose their internal structure. Finally, they were coated with a gold layer with the Gold Coater JFC-1300 (JEOL) for 120 s to 20 mA before scanning. INS COME E' STATO CALCOLATA LA POROSITA'

2.8.2 Confocal microscopy

Confocal microscopy analysis was performed using a Confocal Laser Scanning Biological Microscope Olympus FluoView FV10i to investigate the protein distribution in the hydrogel after coating. To this purpose, the Pvfp5β was marked with Atto633-NHS probe. The PVA3/kC3 FT1 scaffold was also marked by incubation in 5 mL of 0.25 mg/mL FITC aqueous solution for 2 h. The scaffold was then repeatedly washed with distilled water. The laser excitation for the confocal analysis was set at 470 nm for FITC and at 635 nm for Atto633-NHS, and emission recorded at 519 nm for FITC and at 651 nm for the Atto633-NHS. Both 10× and 60 × water immersion objectives were used.

2.9 Cell culture

NIH-3T3 cell line, which is one of the most widely utilized cell line for biomaterial development studies, was used as a model for cell culture assays. Cells were cultured in DMEM supplemented with 10% BCS, 100 U/mL penicillin, 100 µg/mL streptomycin, 1% L-glutamine and 1% non-essential amino acids at 37°C and 5% CO_2 humidified air. Cells were treated with trypsin at 80% confluence using the standard protocol and resuspended into new culture flasks. Cells were passaged every third day.

2.10 Cytotoxicity extract test

The biocompatibility of PVA3/kC3 FT1 and PVA3/kC3 FT1-Pvfp5β hydrogels was evaluated on NIH-3T3 cell line by extract test according to International Standard recommendations for biological evaluation of medical devices [18]. The potential cytotoxicity of any released component from the hydrogels was evaluated on NIH-3T3 cells by RealTime-Glo™ MT Cell Viability assay according to the manufacturer's protocol (Promega, Madison, WI, USA). In particular, the PVA3/kC3 FT1 and PVA3/kC3

FT1-Pvfp5β hydrogels were incubated aseptically in culture medium (extraction vehicle) for 24 h at 37 °C in 5% CO_2. The ratio of hydrogel to extraction vehicle was 1.25 cm^2/mL. Meanwhile, NIH-3T3 cells ($5x10^3$ cells/well) were seeded in white-walled 96-well plates and incubated at 37 °C and 5% CO_2 humidified air for 24 h in 100 µl of culture medium. Then, 50 µl of the culture medium was replaced with 50 µl of extracted eluents (conditioned medium, CM) supplemented with reagent solutions of the RealTime-Glo™ MT Cell Viability assay. For time-zero measurements, cells were incubated with RealTime-Glo™ MT Cell Viability reagent for 60 min at 37 °C, and luminescence was measured by a plate-reading luminometer (GloMax Discover System GM3000; Promega, Madison, WI, USA). Luminescence was then measured after 24 and 48h of incubation. Untreated NIH-3T3 cells were used as control, under the same experimental conditions. Cell viability was quantified as the percentage relatively to control. Three independent experiment were performed.

2.11 Cell adhesion and proliferation on PVA3/kC3 FT1 and PVA3/kC3 FT1-Pvfp5β hydrogels

Sterile hydrogel scaffolds were coated with Pvfp5β at room temperature for 16-20 h as described above. After incubation, the hydrogels were thoroughly rinsed with sterile tissue culture–grade D-PBS and soaked with cell culture medium. Each scaffold was then placed into a well of a 24-well tissue culture plate and a small volume of NIH-3T3 cell suspension containing $5x10^3$ cells was directly pipetted onto the surface of the hydrogel in each well for cell seeding. Cell seeded scaffolds were incubated at 37 °C in 5% CO_2 for 2 h to allow the cells to diffuse into and attach onto the scaffold. Subsequently, 500 µl of fresh culture medium was added and NIH-3T3 cells were cultured onto the hydrogel for 24 h. After that, cell seeded scaffolds were transferred in a white-walled 96-well plates and incubated with RealTime-Glo™ MT Cell Viability reagent for 1 h at 37 °C, and luminescence was measured (time-zero measurements) by GloMax Discover microplate reader in luminescence. Thus, only cells that were attached onto the scaffold were counted for the comparison of cell numbers.

Luminescence was then measured at 24 h and 48 h after the addition of RealTime-Glo™ reagent for cell proliferation determination.

2.12 Viability and morphology of cells cultured on hydrogels

NIH-3T3 cells viability on scaffolds was assessed by the LIVE/DEAD® Viability/Cytotoxicity Kit containing calcein-AM and ethidium homodimer 1 (EthD-1) to see live and dead cells in 3D matrix according to the manufacturer's protocol (Molecular Probes™, Invitrogen, UK). NIH-3T3 cell seeded scaffolds were prepared with $28x10^3$ cells as described above. The cell seeded scaffolds were cultured for 7 days (T7) and 14 days (T14). NIH-3T3 encapsulating scaffolds were thoroughly rinsed with D-PBS and incubated at room temperature for 45 min in a EthD-1 (4.0μM) and calcein-AM (2.0μM) in D-PBS solution. Labeled cells were then viewed under the Nikon Eclipse 80i microscope fluorescence and recorded by a digital camera system. Viable cells were stained with calcein-AM (green), while dead cells were stained with EthD-1 (red).
To assess cell morphology, NIH-3T3 cell seeded scaffolds cultured at T7 and T14 were analyzed by actin filament staining using the green fluorescent Alexa FluorTM 488 Phalloidin (Invitrogen). In these experiments, hydrogels coated with Cell-Tak (BD Bioscience), a natural extract of mfps, or poly-L-lysine (PLL) were also used. Coating was performed as Pvfp5β by adsorption of 0.16 mg/mL Cell-Tak or PLL solution, which were prepared diluting the Cell-Tak protein mixture dissolved in 5% acetic acid, and PLL with Milli-Q water. Briefly, cell seeded scaffolds were fixed in 4% (w/v) paraformaldehyde (PFA) for 20min, washed twice with D-PBS, and permeabilized with 0.5% (v/v) Triton X-100 in D-PBS for 10 min. Samples were blocked for 30 min with 5% normal goat serum (Sigma-Aldrich), 0.1% Triton X-100 in D-PBS. Alexa Fluor™ 488 Phalloidin (1:250) in blocking solution was added and incubated for 1h in the dark. Then, cells were rinsed twice with D-PBS and stained with Hoechst 33342 fluorescent DNA-binding dye at 0.01 mg/mL at room temperature for 10 min. After washing with D-PBS, scaffolds were removed from wells and placed with cell-seeded side facing up, into 8-well chambered coverglass (#155411 ThermoFisher) or on microscope slide for confocal or epifluorescence microscope inspection, respectively. The nuclear

morphology and cytoskeleton were observed on a Nikon Eclipse 80i microscope equipped for epifluorescence or a Confocal Laser Scanning Biological Microscope Olympus FluoView FV10i. Stacks of confocal images were obtained in Z-direction from top to bottom up to 50 μm via Z-stack function of confocal microscopy.

2.13 Statistical analysis

All values reported were obtained as the mean of at least three independent experiments ± Standard Deviations (SD). Results were compared using one-way analysis of variance with pairwise comparisons among treatments made using t-test. The analyses were performed using the Excel software. Results were considered statistically significant at $*p < 0.05$.

3. Results and discussion

3.1 Hydrogel scaffold swelling and erosion behaviour

PVA/kC hydrogels were prepared through a two-steps physical gelation process from the sol-state. kC forms a first network upon cooling the solution from 80 °C to below 50-60 °C when kC chains undergo a conformational transition from coils to coaxial double helices and side-by side dimers of helices (disorder-order transition) [16]. These dimers can also pack side-by-side forming flat ribbons and membranes. This first network incorporates the PVA-containing aqueous phase. In a second step, freeze-thawing is performed to promote PVA crosslinking. The formation of ice crystals causes a local increase of concentration which induces, in turn, PVA crystallization. The PVA crystalline domains remain intact upon thawing, acting as crosslinking points for the PVA network [19]. A schematic representation of scaffold production is shown in Fig. 1.

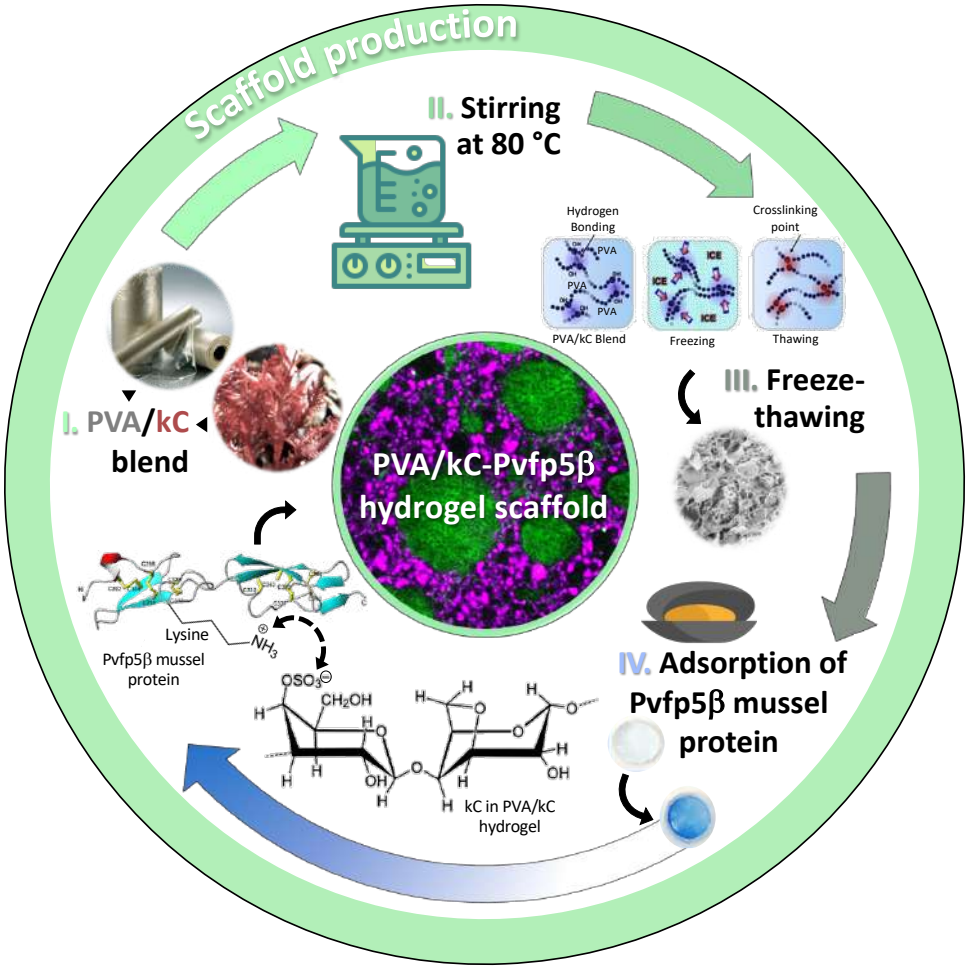

Fig. 1 Schematic representation of scaffold production: I) preparation of the blend of PVA and kC solution at 6 %w total polymer concentration and 1:1 weight ratio of the two components; II) the mixture is stirred at ca. 80 °C until complete homogenization; III) samples were subjected to two freeze-thaw (FT) cycles, each consisting in 2 h dwell at -20 °C and 2 h dwell at room temperature; IV) hydrogel scaffolds are placed into a sterile 96-well tissue culture plate filled with 120 μL of 0.16 mg/mL Pvfp5β solution, the protein is absorbed through interaction between its lysine $-NH_3^+$ and the kC $-SO_3^-$ groups.

The hydrolytic stability of the hydrogel scaffold was evaluated by immersing the films in PBS at 37 °C and following mass variation over time. The samples were also visually inspected to verify their integrity during the prolonged immersion in the PBS buffer. The mean percentage mass change (%MC) as a function of the incubation time and images of representative samples before testing and after being taken out from the incubation bath at given time points are shown in Fig. 2A**.** Initially, the system rapidly swells and %MC after 2 h is +50 but, soon after, the samples start to reduce their weight, reaching negative %MC values after about 3 days. A significant, progressive decrease in sample diameter is also observed (from ~8 mm to ~3 mm), that is not accompanied by an equally significant reduction in thickness (~2 mm), evidence that underlies an inherent anisotropy in the gel microstructure.

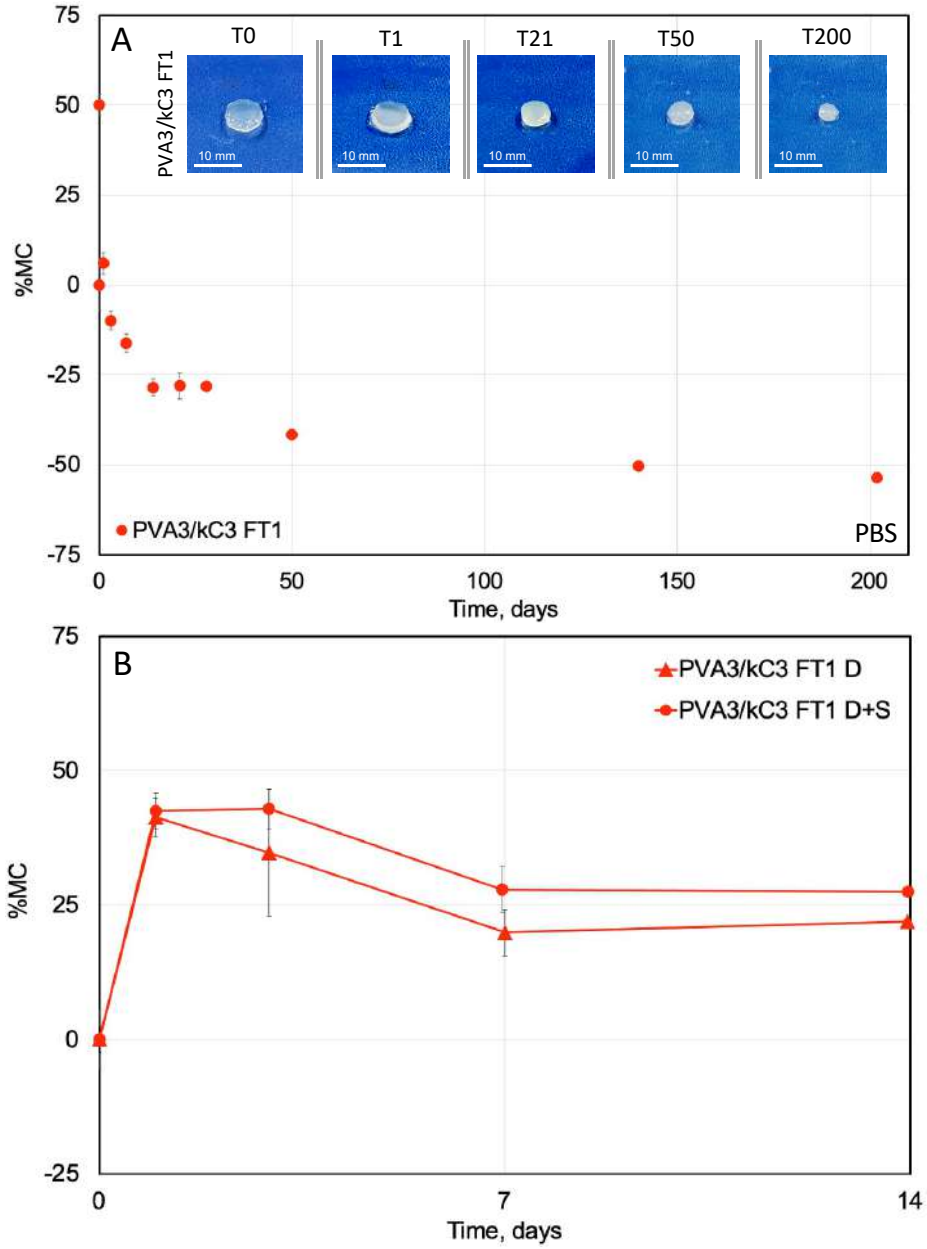

Fig. 2 A) Mean percentage mass change (%MC) as a function of the immersion time in PBS at 37 °C and photographs at various points in time of the swelling/erosion test (T0: 0 days, T1:1 day, T21: 21 days, T50: 50 days and T200: 200 days) in PBS at 37 °C (scale bar 10 mm); B) Mean percentage mass change (%MC) as a function of the immersion time in DMEM (D) and DMEM supplemented with 10% BCS (D+S) at 37 °C.

Hydrogel erosion due to hydrolytic degradation depends on several factors; the chemical nature of the chains that form the network (i.e., presence of hydrolysable

functional groups), the organization of the polymer chains (number and density of crosslinks), the degree of swelling and transport properties of eventual other solutes present in the continuous phase that swells the network. PVA does not possess degradable functional groups with a hydrolytic mechanism. The degradation of this polymer can only occur through oxidative processes catalyzed by enzymes (oxidase and hydrolase) or by suitable reagents (*i.e.*, Fenton reagents) [20]. On the contrary, kC is a polysaccharide that is subjected to hydrolytic degradation at low pH. It can also be efficiently degraded by the glycoside hydrolases found in marine bacteria involved in recycling algal biomass [21], but by none of the enzymes present in human biological fluids, even in the gastro-intestinal tract. In conclusion, under the experimental conditions that are of interest in the view of the application of hydrogels as scaffolds for tissue engineering, neither PVA nor kC should be subjected to degradation. The observed weight decreases with increasing the immersion time in PBS can be then attributed to the erosion of chains and portions of the network that are weakly bound to the others. Hydrogels allow water to breach into the matrix and water-soluble or dispersible components to be released. When erosion, rather than hydrolytic degradation is at the base of structure remodeling and scaffold degradation, there is the advantage of not impacting very much on pH or redox state of the microenvironment.

Fig. 2B shows the values of percentage mass change as a function of the incubation time in DMEM (D) and DMEM supplemented with 10% BCS (D+S) to assess the effect of the typical cell culture media on hydrogel swelling and erosion properties. In particular, DMEM is a classic cell culture medium that guarantees the maintenance of suitable physicochemical conditions (pH and osmolarity) and provides the basic nutrients necessary for cell growth (vitamins and amino acids). The addition of serum is generally performed to stimulate cell growth and adhesion to the substrate through hormonal factors.

Differently from the analysis carried out with a large excess of PBS, in this case the volume of the conditioning medium is comparable to the volume of the sample, that is the condition that will be applied for cell cultures. The system absorbs the conditioning media reaching ~+40 %MC after 1 day incubation (T1). Then, it shows a rather

constant %MC (~+25) between T7 and T14 for both D and D+S. It is also worth mentioning that %MC are positive in the whole investigated time range. This is likely due to both the favorable partitioning of some of the less hydrophilic components present in these media toward the hydrogel inner aqueous phase and the lower osmotic pressure imbalance.

3.2 Influence of conditioning media on hydrogel scaffold mechanical properties

The viscoelastic properties of the as prepared hydrogel and the same hydrogel after conditioning for three (T3), seven (T7) and fourteen (T14) days with each of the two culture media were evaluated by small angle oscillatory strain sweep and frequency sweep tests. Indeed, the composition of the swelling medium can influence the structural organization of the polymer chains forming the network, the porosity of the material across the various length scales, its mechanical properties and the evolution of all the above properties with time. The results of the strain sweep measurements are shown in Fig. 3(A and B). The strain limit of the linear viscoelastic region (γ_c) is not significantly affected by the conditioning time or the nature of the conditioning medium. For strain values, lower than γ_c = ~$3x10^{-3}$ (0.3 % strain), the hydrogel structure is intact even after two weeks conditioning in the culture media. G' values are always one order of magnitude higher than G", indicating that the material behaves as a strong gel. The G' values are affected indeed by conditioning time and medium composition, that change the network organization.

The network structure is best characterized by frequency sweep measurements carried out at strain values below the critical strain and constant temperature of 37 °C, as shown in Fig. 3(C and D). In all conditions, the elastic modulus, G', is one order of magnitude higher than the loss modulus, G'', and G′ is only weakly dependent on frequency. The measurements carried out after 3 days and 7 days immersion in DMEM show a noticeable lowering of G' and G'' curves, while after 14 days, G' and G'' values are higher than those measured after 3 days (Fig. 3C). We can argue that the initial softening phase is probably related to the initial increase of the swelling degree, while the partial recovery of G' and G'' values after 14 days is due to a slow structural

reorganization of the network occurring as a result of the activated segmental dynamics during incubation and more efficient screening of kC negative charges by the cations present in the conditioning medium.

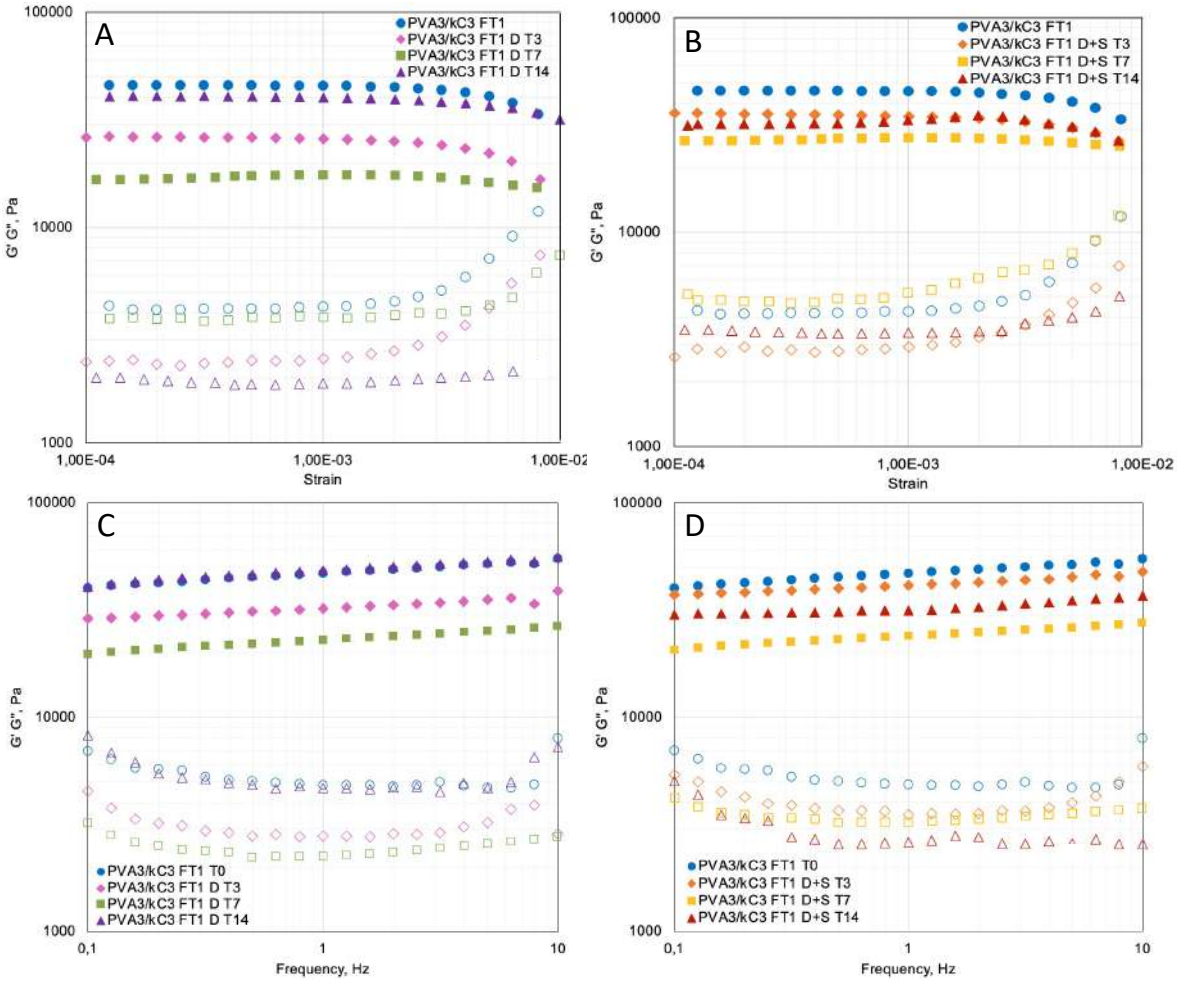

Fig. 3 Storage modulus, G' (full circle), and loss modulus, G" (empty circle), as function of the strain (A-B) and frequency (C-D) of the as prepared hydrogel and hydrogel swollen in DMEM (marked as D) or DMEM with 10% BCS (D+S) for 3 days (T3), 7 days (T7) or 14 days (T14).

The presence of serum in the conditioning medium can cause a further perturbation of the interactions landscape (Fig. 3D). BCS contains hundreds of proteins, the most abundant being albumin. After 14 days of incubation, differently than in PBS, the

process of structural reorganization has only partially restored the elastic properties of the network.

3.3 Adsorption of Pvfp5β onto PVA3/kC3 FT1 scaffold

Cell-surface interaction is a basic requirement for cell survival and functions. Accordingly, the enrichment of 3D scaffolds with bioactive molecules may improve cell adhesion. In this study, recombinant Pvfp5β, a nontoxic adhesive protein that promotes enhancement of cell adhesion [13], was used to functionalize PVA3/kC3 FT1 scaffold. The coating was carried out in an acidic environment by simple adsorption of the cationic Pvfp5β to the negatively charged hydrogel scaffold. Actually, the abundance of lysine residues (9,7%), positively charged (NH_3^+), in Pvfp5β with a pI=9.16 may promotes the formation of electrostatics bonds with the negatively charged (SO_3^-) k-carrageenan in the scaffold. After incubation, the successful adsorption was evaluated measuring the amount of unbound Pvfp5β in solution measured by BCA protein assay. As shown in **Fig. 4A**, approximately 50% of protein was bound to the scaffold. The bound protein was visualized by Coomassie blue staining that colored blue the PVA3/kC3 FT1-Pvfp5β scaffold, while the PVA3/kC3 FT1 (**Fig. 4B**) remained colorless. The integrity of Pvfp5β in the coating solution before (input) and after adsorption (unbound) was evaluated by SDS-PAGE (**Figure 4C**). Our data proved that the adhesive protein Pvfp5β is able to bind efficiently and stably the PVA3/kC3 FT1 scaffold.

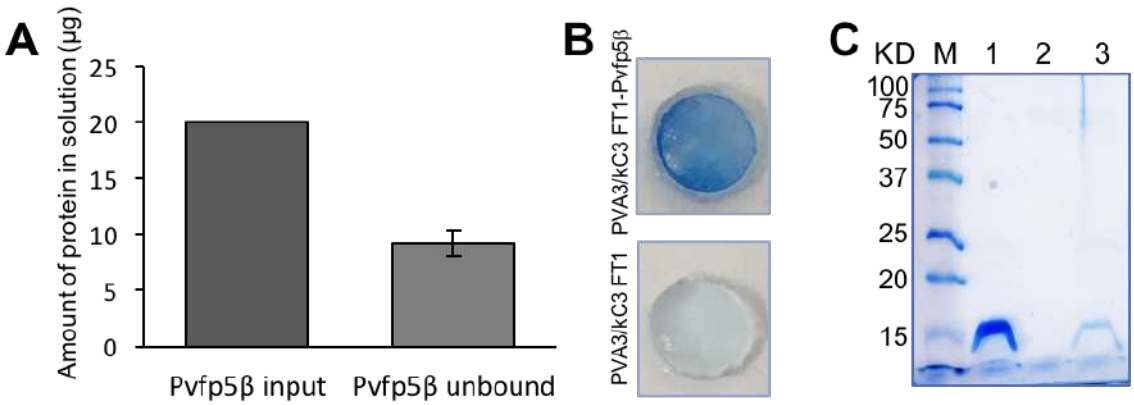

Fig. 4 Analysis of Pvfp5β binding to PVA3/kC3 FT1. (A) Amounts of Pvfp5β used for coating (Pvfp5β input) and Pvfp5β unbound after incubation with scaffold, measured by BCA protein assay. Data are presented as the mean ± SD of three independent experiments; (B) Coomassie blue staining of PVA3/kC3 FT1 coated with Pvfp5β (PVA3/kC3 FT1-Pvfp5β) or uncoated (PVA3/kC3 FT1); (C) SDS-PAGE. 1, Pvfp5β input; 2, negative control (only solvent for binding); 3, Pvfp5β unbound.

The SEM morphology of the as prepared hydrogel, the hydrogel coated with the protein (PVA3/kC3 FT1-Pvfp5β) or treated only with the solvent that is used for the coating process are shown in Fig. 5.

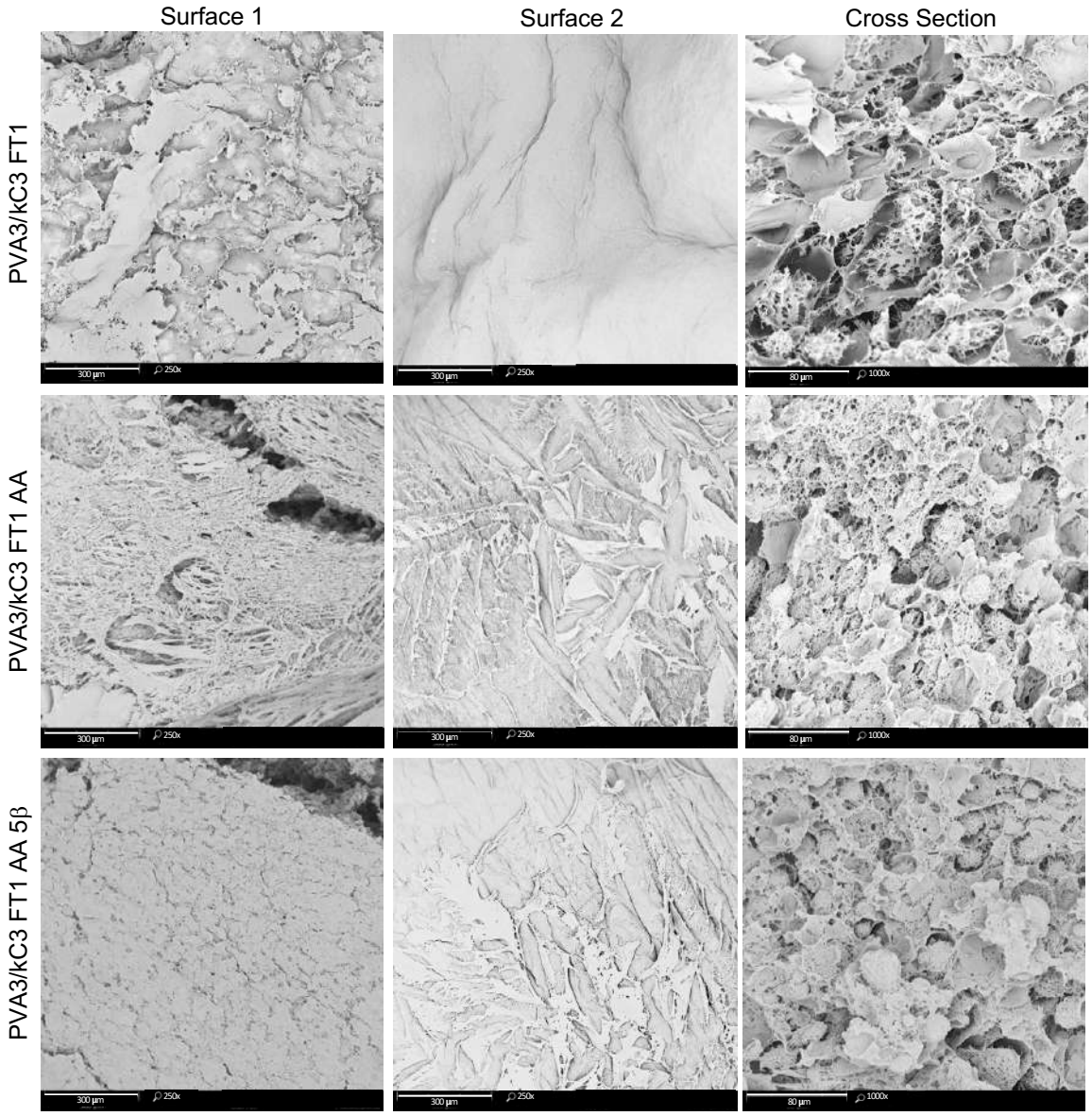

Fig. 5 SEM images of PVA3/kC3 FT1 as prepared, after 1 day immersion in 0.6 %v acetic acid solution (PVA3/kC3 FT1-AA), after 1 day immersion in 0.6 %v acetic acid solution with 0.16 mg/mL Pvfp5β (PVA3/kC3 FT1-Pvfp5β) at 250x magnification for the surfaces and 1000x magnification for the cross sections.

The SEM micrographs show that the two surfaces of the hydrogels are quite dissimilar. One has always a more compact morphology, probably the one in contact to the petri dish during preparation, while the other is more porous. The cross sections of the films present a composite microstructure with a honeycomb morphology with a porosity of

ca. 40 μm; large cells are filled by a "sponge-like" component characterized by much smaller porosity of ca. 3 μm. This morphology is in good agreement with the hypothesis of the formation of two independent networks. The large cell honeycomb structure is likely to be formed by kC, while the incorporated small porosity network is closely resembling those of PVA cryogels [22]. Comparing the different cross sections, we can see that the acetic acid has a mainly shrinking effect without significant modification of the overall structural organization of the two networks. The presence of the protein does not seem to affect the morphology in comparison to the control system treated with only the acetic acid solution.

In order to assess the penetration dept of the protein coating the hydrogel scaffold was subjected to confocal microscopy analysis. For this characterization, the scaffold was impregnated with a FITC containing aqueous solution with the aim to preferentially label PVA, via both isothiocyanate – hydroxyl group reaction and hydrophobic interactions. Indeed, PVA networks form hydrophobic pockets that where amphiphilic molecules can be hosted [23] thus it as more affinity with the FITC while kC containing 3.6-anhydro-D-galactose as part of the repeating unit and fewer sulphate groups than other types of carrageenan is less hydrophilic and less soluble. The protein, in turn, was labelled with Atto 633-NHS.

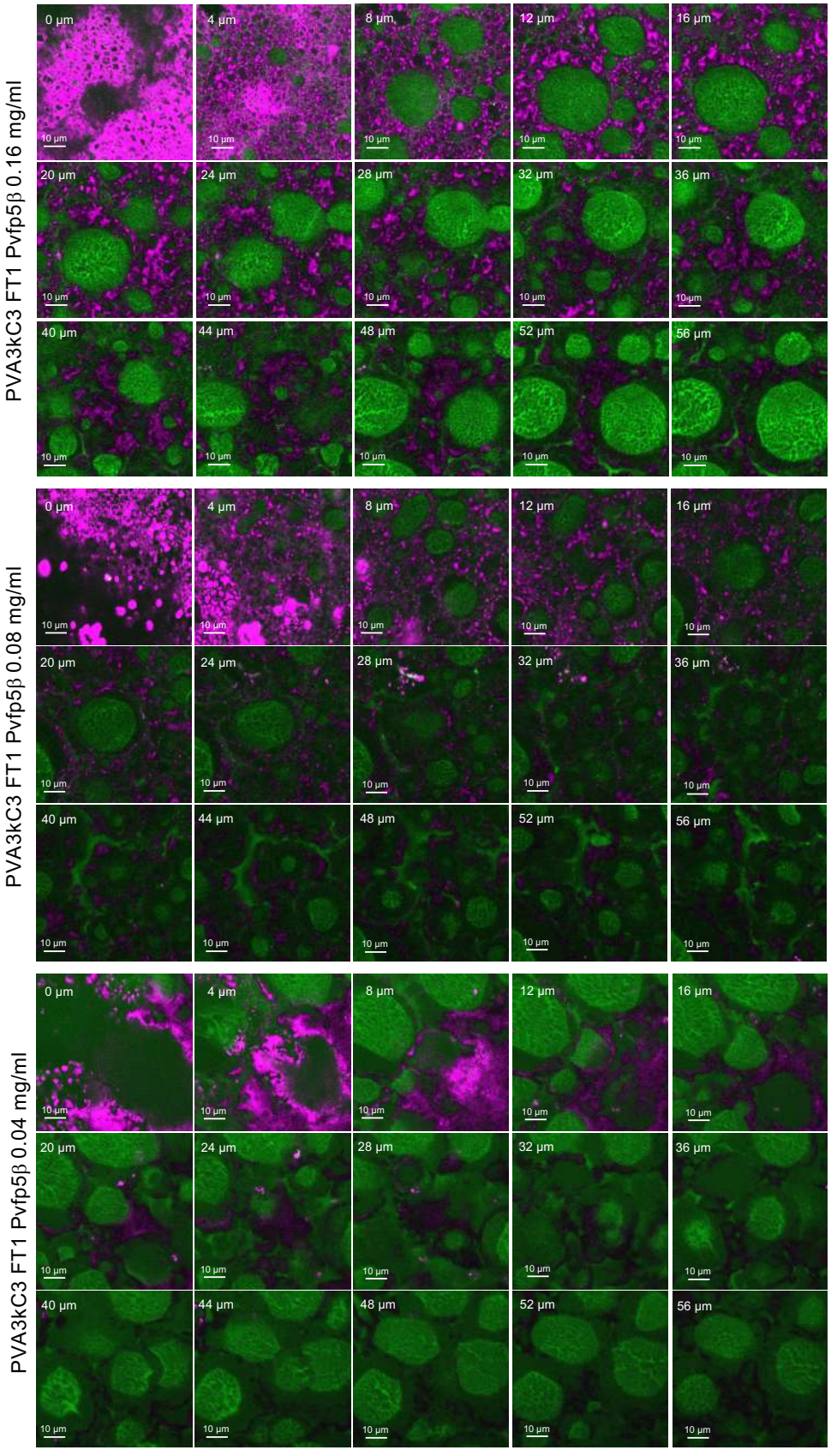
PVA3kC3 FT1 Pvfp5β 0.16 mg/ml
PVA3kC3 FT1 Pvfp5β 0.08 mg/ml
PVA3kC3 FT1 Pvfp5β 0.04 mg/ml
0 µm
4 µm
8 µm
12 µm
16 µm
20 µm
24 µm
28 µm
32 µm
36 µm
40 µm
44 µm
48 µm
52 µm
56 µm
10 µm

Fig. 6 Confocal laser scanning microscopy (CLSM) images of PVA3/kC3 FT1 (green) coated with 0.16 mg/mL, 0.08 mg/mL and 0.04 mg/mL Pvfp5β (pink).

Fig. 6 shows the Pvfp5β scaffold penetration with a protein concentration of 0.16 mg/mL, 0.08 mg/mL and 0.04 mg/mL after 1 day determined by optical slice in the Z-direction, from top to bottom up to 56 μm depth, using confocal microscopy. The protein (pink) is more concentrated on the surface of the hydrogel scaffold and progressively less in the deeper layers although still present to a depth of 56 μm. As the FITC labels mainly the PVA, here it confirms the PVA prevalence in the porous isolated sponges (in green), while the lightly green marked honeycomb structure can be identified as kC. Hence, we can assert that the protein shows a marked preference for kC, avoiding the sponge-like spheres (PVA) that fill the honeycomb cells. The affinity with kC can be explained on the basis of electrostatic interaction with the anionic polysaccharide, being the protein positively charged in acetic acid solution. On the other hand, PVA is often used as anti-fouling hydrogel coating of membranes and biosensors [24]. Reducing the concentration of the protein in the coating solution to 0.08 mg/mL and 0.04 mg/mL corresponds to a lower penetration depth.

3.4 3D Cell culture studies

Preliminarily to any other characterisation, the absence of cytotoxic effects induced by PVA3/kC3 FT1 and PVA3/kC3 FT1-Pvfp5β scaffolds was investigated. This evaluation was performed by using RealTime-Glo™ MT Cell Viability assay and evaluating the effects of conditioned media (CM), containing the eluents extracted from scaffold, on NIH-3T3 fibroblasts, one of the most widely utilized cell lines for biomaterial development studies. As shown in Fig. 7A the extract test revealed that NIH-3T3 cells stayed viable upon exposure to the released components from PVA3/kC3 FT1 or PVA3/kC3 FT1-Pvfp5β scaffolds. Moreover, significant difference in cell viability was observed with PVA3/kC3 FT1_CM at 24 h of exposure versus control group and with both PVA3/kC3 FT1_CM and PVA3/kC3 FT1-Pvfp5β_CM after 48 h, indicating a

positive effect on cell proliferation of the released components from PVA3/kC3 FT1 hydrogel in the extraction medium.

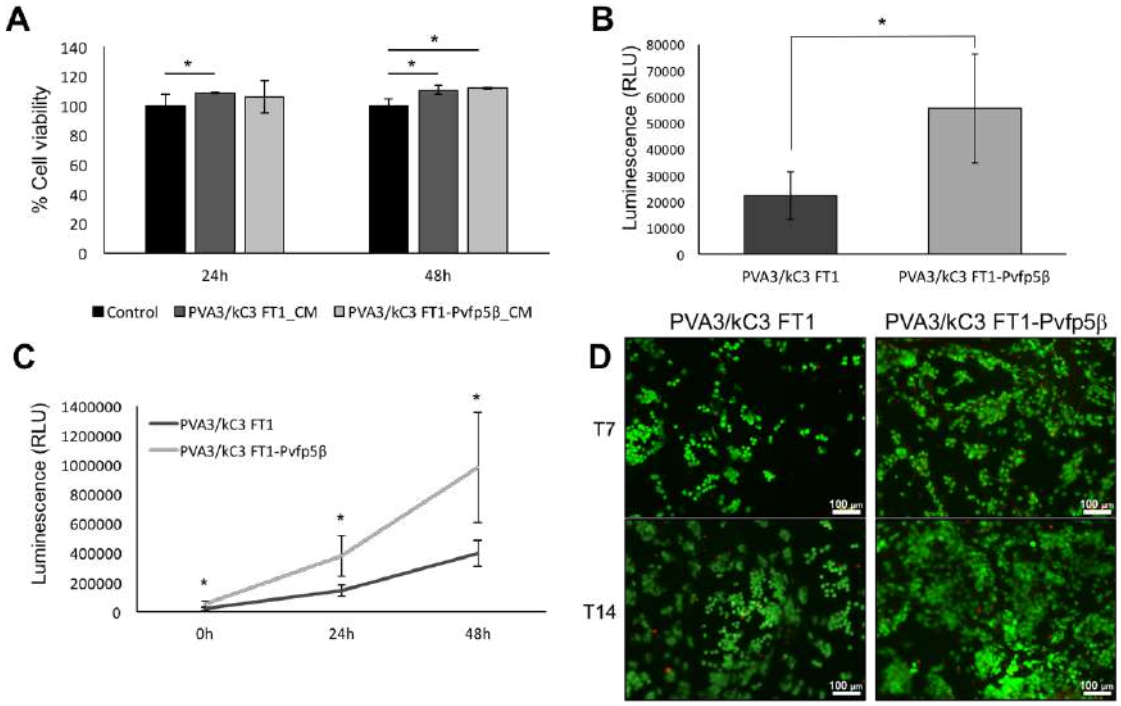

Fig. 7 Cytotoxicity and in vitro cell behavior. (A) Effects of PVA3/kC3 FT1 or PVA3/kC3 FT1- Pvfp5β conditioned media (CM) on NIH-3T3 cell viability after 24 and 48 h of exposure. (B) NIH-3T3 cell adhesion on PVA3/kC3 FT1 and PVA3/kC3 FT1- Pvfp5β scaffolds. Bars indicate relative luminescent units (RLU) of viable cell attached in PVA3/kC3 FT1 (dark gray bar) and PVA3/kC3 FT1-Pvfp5β (light gray bar). (C) NIH-3T3 cell proliferation in PVA3/kC3 FT1 and PVA3/kC3 FT1-Pvfp5β. Relative luminescent units (RLU) of viable cells at 0 time, 24 and 48h of growth. Data are presented as the mean ± SD of three independent experiments. * $p<0.05$. (D) Cell viability of NIH-3T3 cells on PVA3/kC3 FT1-Pvfp5β and PVA3/kC3 FT1 scaffolds at 7 (T7) and 14 (T14) days post seeding, evaluated by Live/Dead assay. Live (green) and dead (red) cells were stained with calcein-AM and EthD-1, respectively. Original magnification 10x. Scale bar 100 µm.

NIH-3T3 fibroblasts were also used to investigate cell adhesion, proliferation, viability and morphology when seeded on PVA3/kC3 FT1 and PVA3/kC3 FT1-Pvfp5β scaffolds.

In particular, cell seeded scaffolds were incubated with RealTime-Glo Viability reagents to quantify the number of attached cells on the scaffolds. As shown in Fig. 7B, an almost twofold increase of cell number was observed on PVA3/kC3 FT1-Pvfp5β scaffold in comparison with PVA3/kC3 FT1, supporting the active role of the Pvfp5β in promoting cell attachment. Cell behaviour of adhered cells onto both scaffolds was then monitored for further 48 h to evaluate if the hydrogel matrix supported cell growth and proliferation. Fig. 7C shows the recorded luminescence measuring living cells in both scaffolds after 24 h and 48 h of growth. The results indicate that NIH-3T3 fibroblasts proliferate in both PVA3/kC3 FT1 and PVA3/kC3 FT1- Pvfp5β scaffolds. The higher number of viable cells present on PVA3/kC3 FT1- Pvfp5β scaffold, both at 24 h and 48 h, indicates that coating with Pvfp5β allows cells to proliferate besides to attach. Cell viability was also measured and traced by live/dead staining of NIH-3T3 cells after 7 days (T7) and 14 days (T14) from seeding onto scaffolds. The results, shown in Fig. 7D, confirm that cells were viable, with a negligible number of dead cells in both scaffolds. More abundant and evenly distributed living cells were found in PVA3/kC3 FT1-Pvfp5β compared with PVA3/kC3 FT1 in agreement with the superior performance in terms of initial cell adhesion. Survival and infiltration of cells inside the scaffolds are major challenges in tissue engineering. Therefore, cell infiltration and morphology of NIH-3T3 at T14 of culture in the 3D scaffolds was determined by optical slicing in the Z-direction, from top to bottom to 51 μm depth, using confocal microscopy. Cell nuclei were stained with Hoechst (blue) while cell morphology was detected by fluorescent phalloidin that stains actin filaments, essential elements in maintaining and modulating cellular morphology. The results, shown in Fig. 8, demonstrate the successful infiltration of cells up to 51 μm in both scaffolds indicating their suitability for cell growth.

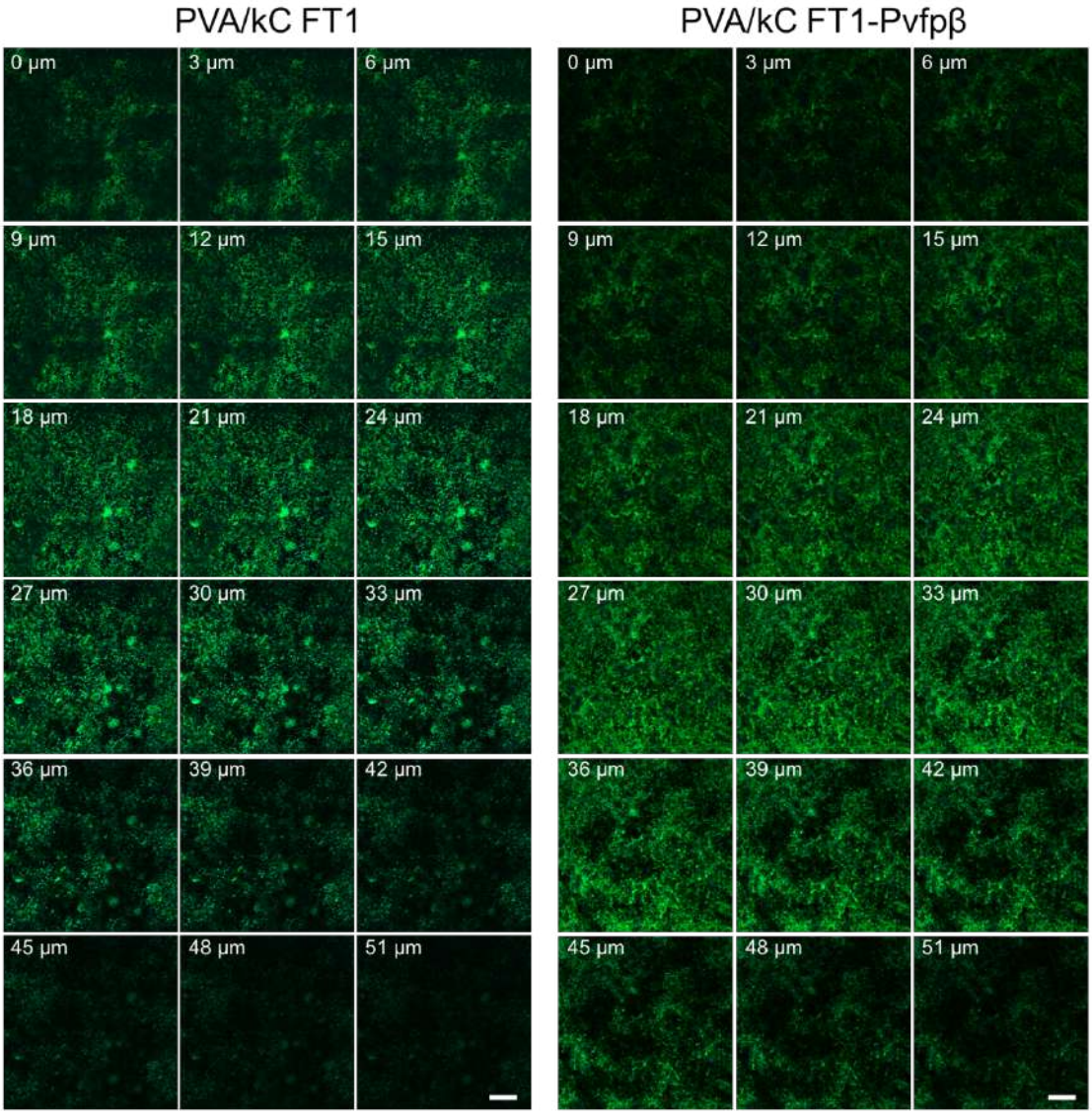

Fig. 8 NIH-3T3 cell infiltration in three-dimensional (3D) PVA3/kC3 FT1 and PVA3/kC3 FT1-Pvfp5β scaffolds. Confocal laser scanning microscopy (CLSM) images of NIH-3T3 cells cultured on PVA3/kC3 FT1 and PVA3/kC3 FT1-Pvfp5β at T14 and stained with Hoechst (nuclei, blue) and Alexa Fluor™ 488-labeled phalloidin (F-actin, green). The merged images, from surface to bottom, of Z-stack images (3 µm each stack, 51 µm deep into the scaffold) are presented. Images were taken with an Olympus FluoView FV-10i laser scanning microscope. Original magnification 10x. Scale bar represents 200 µm.

To further assess the health conditions of NIH-3T3 cells by closely inspecting their morphology on both the 3D scaffolds, Z-stack images were also taken at higher magnification (150x). As shown in Fig. 9, cellular spreading is more evident in PVA3/kC3 FT1-Pvfp5β scaffold with respect to PVA3/kC3 FT1. Therefore, it appears that Pvfp5β could provide contact guidance for cell spreading inside the PVA3/kC3 FT1 scaffold.

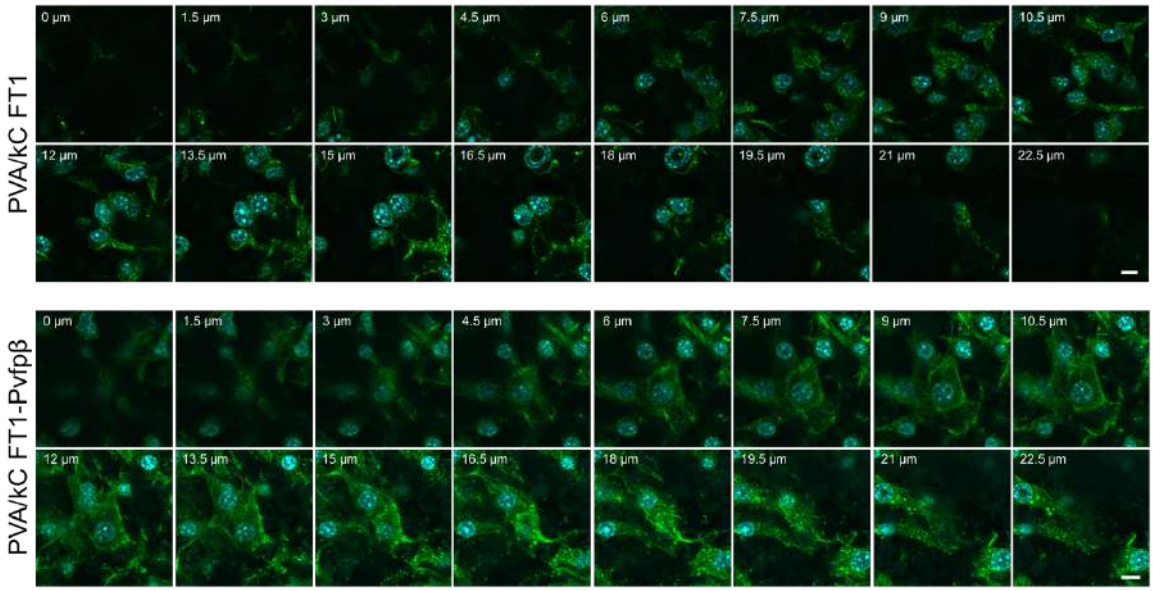

Fig. 9 NIH-3T3 cell infiltration in three-dimensional (3D) PVA3/kC3 FT1 and PVA3/kC3 FT1-Pvfp5β scaffolds. CLSM images of NIH-3T3 cells cultured on PVA3/kC3 FT1 and PVA3/kC3 FT1-Pvfp5β at T14 and stained with Hoechst (nuclei, blue) and Alexa Fluor™ 488-labeled phalloidin (F-actin, green). The merged images, from surface to bottom, of Z-stack images (1.5 µm each stack, 22.5 µm deep into the scaffold) are presented. Images were taken with an Olympus FV-10i laser scanning microscope. Original magnification 150x. Scale bar represents 10 µm.

Finally, we also tried to coat PVA3/kC3 FT1 scaffold with Cell-Tak, a natural extract of the *Mytilus edulis* adhesive-protein mixture of mfp-1 and -2, and with poly-L-lysine (PLL), generally used to coat tissue culture plates or surfaces for enhancing cell attachment. Fig. 10A shows NIH-3T3 cells seeded on PVA3/kC3 FT1 coated with Pvfp5β, Cell-Tak or PLL. Cells were stained with fluorescent phalloidin and with Hoechst. All three coated scaffolds showed higher cell density than the corresponding

uncoated scaffolds treated with only solvent that is water for PLL and 0.6%v acetic acid for Cell-Tak and Pvfp5β (Fig. 10B). Interestingly, homogeneous cell distribution and higher cell number were observed on PVA3/kC3 FT1-Pvfp5β than in PVA3/kC3 FT1-CellTak and PVA3/kC3 FT1-PLL.

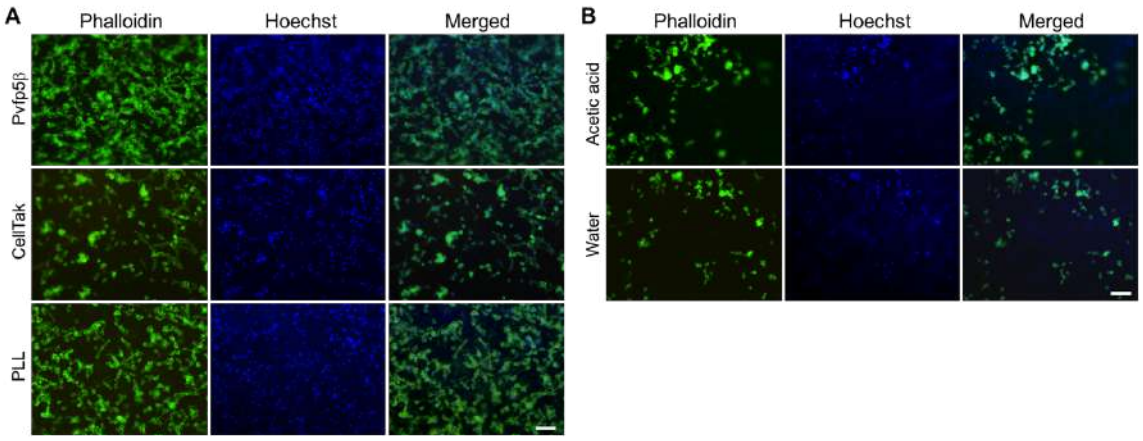

Fig. 10 Representative fluorescence images of NIH-3T3 cells at day 7 post seeding on coated PVA3/kC3 FT1 with Pvfp5β, Cell-Tak or PLL (A) or with only solvent, water or 0.6%v acetic acid (B). Cell nuclei was in blue (Hoechst staining-DAPI channel) and F-actin was in green (Alexa Fluor™ 488-labeled phalloidin staining-FITC channel). Images were taken with a Nikon Eclipse 80i microscope equipped for epifluorescence. Scale bar 100 μm.

In conclusion, the recombinant Pvfp5β successfully binds the PVA3/kC3 FT1 hydrogel improving cell-surface interaction and cytoskeleton reorganization of NIH-3T3 cells leading to a more evident cellular spreading. The molecular mechanisms that regulate the NIH-3T3 behaviour on PVA3/kC3 FT1-Pvfp5β need to be still clarified and will be the object of future investigation. About this, it is interesting to note that Pvfp5β native protein consisting of 82 amino acids has a high homology with two tandem epidermal growth factor (EGF)-like domains. The structural characterization of the recombinant protein Pvfp5β confirmed that it is folded as a β-rich protein with correct pairing of the sulphur bridges according to an EGF-like module [25,13]. EGF plays an important role in the regulation of cell growth, migration, proliferation, and differentiation during development and in adult animal by binding to its receptor EGFR [26]. Interestingly,

several molecules of extra-cellular matrix (ECM), such as laminin, tenascin and thrombospondin, contain multiple copies of EGF-like domains. These molecules, also called matrikines, can bind to EGF receptors and signal cell growth directly as organized solid-phase ligands or after release by proteolysis [27,28,29,30,31,32]. Thus, one can speculate that immobilized Pvfp5β could bind to EGF receptor as solid-phase ligand and lead to signal transduction responses by cells though a receptor-mediated binding. In fact, immobilization of growth factors to biomaterial substrates has emerged as a method for improving the stability and persistence of growth factor delivered to cells or tissues [33]. Future studies will be directed to elucidate if soluble and immobilized Pvfp5β can induce EGF receptor autophosphorylation and activation of intracellular signalling pathways as PI3K/AK, ERK/MAPK and PLCγ in several cell types including stem cells of different tissue origins.

4. Conclusions

This work investigated the effect of the biomimetic protein Pvfp5β, used as a coating of a hydrogel scaffold based on a 50 %w mixture of PVA and kC, in promoting cell adhesion, spreading and migration. The scaffold preparation consists in a two-step physical gelation process. From the homogeneous mixture of PVA and kC, a primary network forms upon cooling the solution from 80 °C to room temperature. A second network, from the aqueous PVA entrapped in the cells formed by kC, is obtained by freeze-thawing. The kC-based honeycombed structure preferentially adsorbs the protein, probably due to electric charge interaction. The lack of interaction between Pvfp5β and PVA is in line with anti-biofouling properties of PVA hydrogels. Interestingly, PVA favorably entraps the fluorescent label used to visualize the network by confocal microscopy, probably due to hydrophobic interactions. Penetration of the protein into the scaffold is controlled by the protein concentration in the coating solution. The scaffold slowly erodes with time when incubated in a large excess of isotonic phosphate buffer. It swells and remodels itself when conditioned with small volumes of more complex media such as DMEM and DMEM combined with serum. The uptake of serum proteins allows the scaffold to properly support the cell functions. The

coating process does not appreciably affect the morphology of the scaffold. The recombinant Pvfp5β adsorbed clearly improves cell-surface interaction and cytoskeleton reorganization of NIH-3T3 cells, leading to higher cell adhesion and more effective colonization of the scaffold. The molecular mechanisms that regulate the cells behaviour on PVA3/kC3 FT1-Pvfp5β will be the object of future investigations, although it could be probably anticipated that the epidermal growth factor (EGF)-like domains of protein play a role in enhancing cell adhesion and proliferation.

CRediT authorship contribution statement

Emanuela Muscolino: Investigation, Writing - Original Draft. **Maria Assunta Costa:** Investigation, Writing - Original Draft. **Maria Antonietta Sabatino:** Methodology, Supervision. **Sabina Alessi:** Methodology, Supervision. **Donatella Bulone:** Conceptualization. **Pier Luigi San Biagio:** Conceptualization. **Rosa Passantino:** Conceptualization, Supervision, Writing - Review & Editing. **Daniela Giacomazza:** Supervision, Resources, Writing - Review & Editing. **Clelia Dispenza:** Conceptualization, Resources, Funding acquisition, Writing - Review & Editing. All Authors have reviewed and approved the final manuscript.

Declaration of competing interest

The authors declare that there are no conflicts of interest.

Funding

This work was supported by the European Social Assets "Sicilia 2020 – Rafforzare l'occupabilità nel sistema R&S e la nascita di Spin Off di ricerca in Sicilia" (P.O. FSE 2014/2020 Project - CUP: G77B17000220009) and by FFR_D09-Fondo di Finanziamento per la Ricerca di Ateneo 2018/2021 (Ref. Clelia Dispenza).

Acknowledgements

The authors wish to thank Alessia Provenzano at CNR IBF and the laboratory of "Bioimaging e Dosimetria" of ATeN Center - University of Palermo, for their valuable technical technical support.

References

[1] K. Klimek, G. Ginalska, Proteins and Peptides as Important Modifiers of the Polymer Scaffolds for Tissue Engineering Applications—A Review, *Polymers* 12 (2020) 844. https://doi.org/10.3390/polym12040844.

[2] B.P. Lee, P.B. Messersmith, J.N. Israelachvili, J.H. Waite, Mussel-Inspired Adhesives and Coatings, Annu. Rev. Mater. Res. 41 (2011) 99-132. https://doi.org/10.1146/annurev-matsci-062910-100429.

[3] Q. Guo, J. Chen, J. Wang, H. Zeng, J. Yu, Recent progress in synthesis and application of mussel-inspired adhesives, Nanoscale 12 (2020) 1307-1324. https://doi.org/ 10.1039/c9nr09780e.

[4] L.M. Rzepecki, K.M. Hansen, J.H. Waite, Characterization of a Cystine-Rich Polyphenolic Protein Family from the Blue Mussel Mytilus edulis L, Biol. Bull. 183 (1992) 123-137. https://doi.org/ 10.2307/1542413.

[5] J. Yu, W. Wei, E. Danner, R.K. Ashley, J.N. Israelachvili, J.H. Waite, Mussel protein adhesion depends on interprotein thiol-mediated redox modulation, Nat. Chem. Biol. 7 (2011) 588-90. https://doi.org/10.1038/nchembio.630.

[6] S.C. Daubner, T. Le, S. Wang, Tyrosine hydroxylase and regulation of dopamine

synthesis, Arch. Biochem. Biophys. 508 (2011) 1-12. https://doi.org/10.1016/j.abb.2010.12.017.
[7] P.K. Forooshani, B.P. Lee, Recent approaches in designing bioadhesive materials inspired by mussel adhesive protein, J. Polym. Sci. A Polym. Chem. 55 (2017) 9-33. https://doi.org/10.1002/pola.28368.
[8] J.P. Gallivan, D.A. Dougherty, A Computational Study of Cation−π Interactions vs Salt Bridges in Aqueous Media: Implications for Protein Engineering, J. Am. Chem. Soc. 122 (2000) 870-874. https://doi.org/10.1021/ja991755c.
[9] N. Pandey, L.F. Soto-Garcia, J. Liao, P. Zimmern, K.T. Nguyen, Y. Hong, Mussel-inspired bioadhesives in healthcare: design parameters, current trends, and future perspectives, Biomater. Sci. 8 (2020) 1240-1255. https://doi.org/10.1039/c9bm01848d.
[10] W. Zhang, R. Wang, Z. Sun, X. Zhu, Q. Zhao, T. Zhang, A. Cholewinski, F.K. Yang, B. Zhao, R. Pinnaratip, P.K. Forooshani, B.P. Lee, Catechol-functionalized hydrogels: biomimetic design, adhesion mechanism, and biomedical applications, Chem. Soc. Rev. 49 (2020) 433-464, https://doi.org/10.1039/c9cs00285e.
[11] S. Hu, X. Pei, L. Duan, Z. Zhu, Y. Liu, J. Chen, T. Chen, P. Ji, Q. Wan, J. Wang, A mussel-inspired film for adhesion to wet buccal tissue and efficient buccal drug delivery, Nat. Commun. 12 (2021) 1689. https://doi.org/10.1038/s41467-021-21989-5.
[12] G.P. Maier, M.V. Rapp, J.H. Waite, J.N. Israelachvili, A Butler. BIOLOGICAL ADHESIVES. Adaptive synergy between catechol and lysine promotes wet adhesion by surface salt displacement, Science 349 (2015) 628-32. https://doi.org/10.1126/science.aab0556.
[13] R. Santonocito, F. Venturella, F. Dal Piaz, M.A. Morando, A. Provenzano, E. Rao, M.A. Costa, D. Bulone, P.L. San Biagio, D. Giacomazza, A. Sicorello, C. Alfano, R. Passantino, A. Pastore, Recombinant mussel protein Pvfp-5β: A potential tissue bioadhesive, J. Biol. Chem. 294 (2019) 12826-12835. https://doi.org/10.1074/jbc.RA119.009531.
[14] P. Bilotto, C. Labate, M.P. De Santo, K. Deepankumar, A. Miserez, B. Zappone, Adhesive Properties of Adsorbed Layers of Two Recombinant Mussel Foot Proteins with Different Levels of DOPA and Tyrosine, Langmuir 35 (2019) 15481-15490. https://doi.org/10.1021/acs.langmuir.9b01730.
[15] X. Ou, B. Xue, Y. Lao, Y. Wutthinitikornkit, R. Tian, A. Zou, L. Yang, W. Wang, Y. Cao, J. Li, Structure and sequence features of mussel adhesive protein lead to its salt-tolerant adhesion ability, Sci. Adv. 6 (2020) eabb7620. https://doi.org/10.1126/sciadv.abb7620.
[16] M.R. Mangione, D. Giacomazza, D. Bulone, V. Martorana, P.L. San Biagio, Thermoreversible gelation of κ-Carrageenan: Relation between conformational transition and aggregation, Biophys. Chem. 104 (2003) 95–105. https://doi.org/10.1016/S0301-4622(02)00341-1.
[17] G. Paradossi, F. Cavalieri, E. Chiessi, Poly(vinyl alcohol) as versatile biomaterial for potential biomedical applications, J. Mat. Sci. – Mat. Med. 14 (2003) 687-691.
[18] ISO10993-5:2009, Biological evaluation of medical devices, part 5: tests for in vitro cytotoxicity. iso.org/standard/36406.html.
[19] W. Wan, A.D. Bannermann, L. Yang, H. Mak, Poly(vinyl alcohol) cryogels for biomedical applications, in: O. Okay, Ed., Polymeric Cryogels, Advances in Polymer

Science 263, Springer International Publishing Switzerland, 2014, pp. 283-321. https://doi.org/10.1007/978-3-319-05846-7_8.
[20] C.C. Lin, K.S. Anseth, (2013). The Biodegradation of Biodegradable Polymeric Biomaterials, in: Biomaterials Science (Third Edition), Elsevier, pp. 716–728. https://doi.org/10.1016/B978-0-08-087780-8.00061-9.
[21] P.N. Collén, M. Lemoine, R. Daniellou, J.P. Guégan, S. Paoletti, W. Helbert, Enzymatic Degradation of κ-Carrageenan in Aqueous Solution, Biomacromolecules, 10 (2009) 1757–1767. https://doi.org/10.1021/bm9001766.
[22] J.L. Valentin, D. Lopez, R. Hernandez, C. Mijangos, K. Saalwachter, Structure of poly(vinyl alcohol) cryo-hydrogels as studied by proton low-field NMR spectroscopy, Macromolecules, 42 (2009) 263-272. https://doi.org/10.1021/ma802172g.
[23] M. Ricca, V. Foderà, D. Giacomazza, M. Leone, G. Spadaro, C. Dispenza, Probing the internal environment of PVP networks generated by irradiation with different sources, Colloid and Polymer Science, 288 (2010) 969–980. https://doi.org/10.1007/s00396-010-2217-7.
[24] J. Liu, S. Qu, Z. Suo, W. Yang, Functional hydrogel coatings, Natl. Sci. Rev. 8 (2021) nwaa254. https://doi.org/10.1093/nsr/nwaa254.
[25] L. Petrone, A. Kumar, C.N. Sutanto, N.J. Patil, S. Kannan, A. Palaniappan, S. Amini, B. Zappone, C. Verma, A. Miserez, Mussel adhesion is dictated by time-regulated secretion and molecular conformation of mussel adhesive proteins, Nat. Commun. 6 (2015) 8737. https://doi.org/10.1038/ncomms9737.
[26] F. Edwin, G.J. Wiepz, R. Singh, C.R. Peet, D. Chaturvedi, P.J. Bertics, T.B. Patel, A historical perspective of the EGF receptor and related systems, Methods Mol. Biol. 327 (2006) 1-24. https://doi.org/10.1385/1-59745-012-x:1.
[27] J. Engel, EGF-like domains in extracellular matrix proteins: localized signals for growth and differentiation? FEBS Lett. 251 (1989) 1-7. https://doi.org/10.1016/0014-5793(89)81417-6.
[28] G. Panayotou, P. End, M. Aumailley, R. Timpl, J. Engel, Domains of laminin with growth-factor activity, Cell 56 (1989) 93-101. https://doi.org/10.1016/0092-8674(89)90987-2.
[29] C.S. Swindle, K.T. Tran, T.D. Johnson, P. Banerjee, A.M. Mayes, L. Griffith, A. Wells, Epidermal growth factor (EGF)-like repeats of human tenascin-C as ligands for EGF receptor, J. Cell Biol. 154 (2001) 459-68. https://doi.org/10.1083/jcb.200103103.
[30] S. Schenk, E. Hintermann, M. Bilban, N. Koshikawa, C. Hojilla, R. Khokha, V. Quaranta, Binding to EGF receptor of a laminin-5 EGF-like fragment liberated during MMP-dependent mammary gland involution, J. Cell Biol. 161 (2003) 197-209. https://doi.org/10.1083/jcb.200208145.
[31] R.O. Hynes, The extracellular matrix: not just pretty fibrils, Science 326 (2009) 1216-9. https://doi.org/10.1126/science.1176009.
[32] J. Grahovac, A. Wells, Matrikine and matricellular regulators of EGF receptor signaling on cancer cell migration and invasion, Lab. Invest. 94 (2014) 31-40. https://doi.org/10.1038/labinvest.2013.132.

[33] K.S. Masters, Covalent growth factor immobilization strategies for tissue repair and regeneration, Macromol. Biosci. 11 (2011) 1149-63. https://doi.org/10.1002/mabi.201000505.